

Comparison of Results of SHRP and Conventional Binder Tests on Paving Asphalts

Ming-Gin Lee^{a*}, Chui-Te Chiu^b, Yu-Cheng Kan^a, and Kuei-Ching Chen^a

^a *Department of Construction Engineering
Chaoyang University of Technology
Taichung County 41349, Taiwan, R.O.C.*

^b *Department of Civil Engineering
Chung-Hua University, Hsinchu 300, Taiwan, R.O.C.*

Abstract: This study was conducted to compare the results of SHRP and conventional binder tests on paving asphalts. The test results indicate that Brookfield viscosity shows a fairly strong correlation with $G^*/\sin \delta$ at high service temperature. Penetration shows a strong correlation with $G^* \times \sin \delta$ at 25°C, and Fraass breaking point shows a moderate relationship with SHRP limiting stiffness temperature. The relationship between the creep stiffness and the failure strain at -12, -18 and -24°C is very good ($R^2=0.81$) as compared with the others. Creep stiffness decreases as failure strain increases. The Bitumen Test Data Chart (BTDC) basically allows one to take different physical property measurements (viscosity, penetration, Fraass temperature, and/or softening point) and predict the consistency of the material over a wide temperature range. Family curves of the BTDC could be used to compare the characteristics of a binder as it ages. A PG grade binder with a wide temperature range will display a low-temperature susceptibility in the BTDC.

Keywords: SHRP, PG grade, Fraass breaking point, BTDC.

1. Introduction

The main goal of the SHRP (Strategic Highway Research Program) Program was to develop pavement performance-based specifications for asphalt binders and mixtures. The specification criteria in a true performance-based specification must be representative of the material in the pavement [1].

In the SHRP Superpave binder specification, the conventional Rolling Thin Film Oven Test (RTFOT) is used to simulate the effects of the hot-mix process on a binder, and the Pressure

Aging Vessel (PAV) is used to simulate additional aging of the binder in service. The SHRP performance-based specifications were to be established on a set of validated relationships among asphalt binder properties, mixture properties and pavement performance that establish acceptable response ranges to control low-temperature cracking, fatigue cracking, permanent deformation (rutting), aging, adhesion, and water sensitivity.

Accelerated laboratory tests and parameters that relate to field performance are used in the specification [1,2]. These include proper-

* Corresponding author; e-mail: mglee@mail.cyut.edu.tw

ties in three different temperature ranges that would be related to pavement rutting, low-temperature cracking, and fatigue cracking. The SHRP asphalt binder specification would allow the engineer to match materials to different levels of pavement service and to make the choice of asphalt binder to resist specific distress mechanisms. The system was to be based upon rational performance indices established for both low and high pavement service temperatures.

Performance grading is based upon the properties of the asphalt binder aged to simulate a specific pavement service life (maybe 5 years). Thus, a precise grade may be selected to fit the need to control low-temperature cracking, fatigue cracking and rutting, or any combination in a particular construction project [2, 3]. However, some researchers [4,5] found that SHRP test parameters, such as $G^*/\sin \delta$ and $G^* \times \sin \delta$, might not necessarily correlate with the performance of the pavement in the field.

Additionally, SHRP PG grades cannot be used to predict or control specific levels of rutting or cracking for different mixtures, pavement structures or environments. Further evaluation of these parameters is needed, especially on their applicability to any local conditions.

The purpose of this study was to compare and find the relationship between results of SHRP binder tests and conventional binder tests on paving asphalts. This study also addressed both the SHRP PG grade and Bitumen Test Data Chart (BTDC) for the asphalt binders as well as the aging characteristics of these binders by means of the rolling thin film oven and pressure aging vessel procedures.

2. Testing program

Six different asphalt binders (conventional and modified) were used in this study. The three types of modifiers used in this study were ground tire rubber, styrene block copolymer and styrene-butadiene rubber. The sty-

rene-butadiene rubber modifiers, which included a low-molecular-weight SBR2 and a high-molecular-weight SBR7, were blended with an AC-10 at a level of 3% by weight of the asphalt to produce the SBR-modified asphalts. The blending of the SBR-modifiers with the asphalt was done by the company which supplied these modifiers. A nominal size #80 ground tire rubber was blended with an AC-30 at a level of 10% by weight of the asphalt in the laboratory. The styrene block copolymer modifier was blended with an AC-20 at a level of 3% by weight of the asphalt to produce the SB-modified asphalt.

The blending of the SB-modifier with the asphalt was done by the company which supplied this modifier. These modified and unmodified asphalts were subjected to the standard RTFOT process to simulate the short-term aging effect that occurs in the hot-mixing process and followed by the SHRP PAV process at 100°C to simulate the additional aging of the asphalt binder in the field.

All of these asphalts and asphalt blends were evaluated by both conventional binder tests and the SHRP binder tests. The following conventional binder tests were performed on the original binders, and on the RTFOT and RTFOT+PAV residues:

1. Penetration test at 25°C (ASTM D5).
2. Brookfield viscosity at 60°C (ASTM D4402).
3. Fraass Breaking Point test (IP80/63).

The Fraass Breaking Point test is routinely used in Europe to evaluate low temperature binder behavior. In this test, a film of asphalt is placed on a thin metal plate, and then is flexed at increasing lower temperatures until the first crack is observed. Comparison of the Fraass temperature to the theoretical cracking temperature shows that the Fraass Breaking Point is usually 16 ~ 19°C above the cracking temperature. This difference is due to the much higher strain rate which is applied to the asphalt in the Fraass Breaking Point test [3].

The SHRP binder tests were performed in

accordance with the procedures for SHRP binder classification. The following SHRP binder tests were performed:

1. Dynamic Shear Rheometer (DSR) test at high service temperatures from 52°C to 8°C on the original binders and RTFOT residues, and at intermediate service temperatures from 13°C to 34°C on the RTFOT+PAV residues.
2. Bending Beam Rheometer (BBR) test at low service temperatures of -12, -18 and -24°C on the RTFOT+PAV residues.
3. Direct Tension Rheometer (DTR) test at low service temperatures of -12, -18 and -24°C on the RTFOT+PAV residues.

3. Results and discussion

Test Results from the conventional binder tests and the SHRP binder tests are listed in Tables 1 and 2, respectively. The discussion and analysis of these results are presented in following sections.

3.1. Binder rheological properties at high service temperature

Asphalt mixtures are more susceptible to rutting and shoving at high service temperature when the mixture has a lower viscosity and is more easy to creep under heavy traffic loading.

At high pavement service temperature when the binder is relatively softer, the strength of the mixture would be predominantly affected by the characteristics of the aggregate. However, when the aggregate factor is fixed, an asphalt binder with a harder stiffness or higher viscosity should give better rutting resistance to the asphalt mixture. For most unmodified and modified asphalts oxidative aging result in increased G^* values and decreased δ values.

These changes result in more resistance to deformation and more elasticity, which means more contribution to rutting resistance. It is reasonable that the SHRP specification has minimum limits of $G^*/\sin \delta$ on the unaged and

the oven-aged binders to control tenderness and rutting.

However, Reese and Goodrich [4] found that $G^*/\sin \delta$ does not explain the rutting which occurred at the laboratory concrete creep test studies and the Needles test road.

Figure 1 shows the plot of Brookfield viscosity at a shear rate of 1 s^{-1} and a temperature of 60°C versus the $G^*/\sin \delta$ at 60°C for all six asphalt binders before and after the RTFOT process. $G^*/\sin \delta$ increases as the viscosity increases. The correlation is quite good ($R^2=0.94$).

3.2. Binder rheological properties at intermediate service temperature

At ambient service temperature, an asphalt binder behaves partially as a solid and partially as a liquid. As an asphalt binder hardens with time, the stiffness of the asphalt concrete would increase. A stiffer asphalt concrete would cause the maximum load-induced stress to increase, and increase the cracking potential of the pavement. Tayebali [7] stated that asphalt-aggregate mixtures with lower stiffness are likely to demonstrate better fatigue resistance under controlled-strain loading than their counterparts with higher stiffness.

Conversely, laboratory stress-controlled fatigue testing implies that stiffer binders are more resistant to fatigue cracking [8]. Some studies also related asphalt stiffness to its penetration value [9-10]. The SHRP binder parameter used for control of the fatigue performance of asphalt binders is the loss modulus, $G^*\sin \delta$, which is measured at the intermediate pavement temperature ranging from 4 to 40°C. It is based on the dissipated energy theory which is directly proportional to the $G^*\sin \delta$ [6]. Figure 2 shows the plot of penetration versus the $G^*\sin \delta$ at 25°C for all six asphalt binders before and after the RTFOT and PAV processes. $G^*\sin \delta$ (loss modulus) increases as the penetration decreases.

The correlation is quite good ($R^2=0.86$).

Table 1. Conventional binder test results

Asphalt binders	Penetration @25 °C (dmm)	Viscosity @60 °C (poise)	Fraass breaking point (°C)
Unaged binder			
AC-10	92.0	1218	-13.3
AC-10+3%SBR2	86.3	2603	-16.8*
AC-10+3%SBR7	78.1	3617	-15.0*
AC-20+3%SB	74.7	7134	-13.8*
AC-30	61.5	3674	-12.3
AC-30+10%CR	44.1	11403	-12.5*
RTFOT residue			
AC-10	52.5	6276	-12.0
AC-10+3%SBR2	51.7	12889	-14.8*
AC-10+3%SBR7	51.4	17222	-13.8*
AC-20+3%SB	44.2	16774	-12.5*
AC-30	36.0	10849	-11.3
AC-30+10%CR	36.0	43937	-11.3
PAV+RTFOT residue			
AC-10	31.9	26376	-9.0
AC-10+3%SBR2	29.3	48660	-12.5*
AC-10+3%SBR7	27.1	53040	-12.5*
AC-20+3%SB	28.0	38946	-10.8
AC-30	22.8	80650	-8.8*
AC-30+10%CR	19.0	310481	-9.7*

Note: * means the first micro-crack.

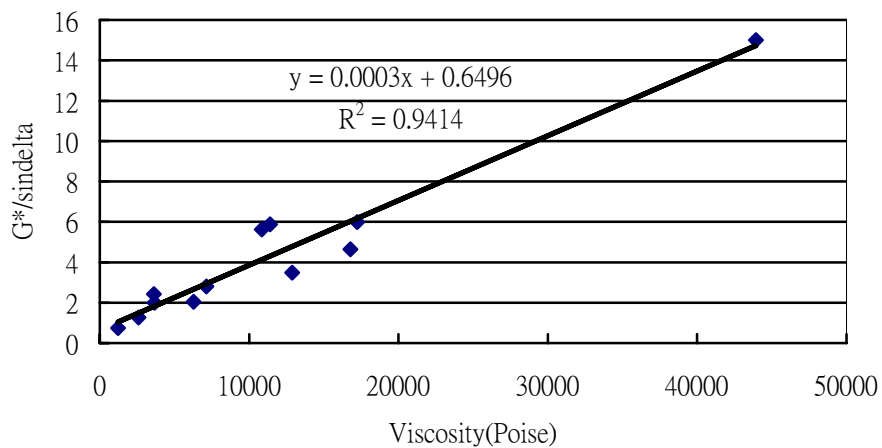


Figure 1. Relationship between brookfield viscosity and $G^*/\sin\delta$ at 60°C

Table 2. Results of SHRP classification testing of asphalt binders

Asphalt binders	AC-10	AC-10+ 3%SBR2	AC-10+ 3%SBR7	AC-20+ 3%SB	AC-30	AC-30+ 10%CR
Tests on unaged binder (w=10rad/s)						
Brookfield,135°C, Pas	0.200	0.263	0.516	0.598	0.566	1.055
Flash point,°C	273	278	280	272	295	310
G*/sin δ @52°C, kPa	4.09	6.17	10.41	12.76	9.79	27.22
G*/sin δ @58°C, kPa	1.61	2.64	5.31	5.67	4.05	13.94
G*/sin δ @64°C, kPa	0.74	1.27	2.42	2.81	2.00	5.88
G*/sin δ @70°C, kPa	0.36	0.67	1.13	1.50	0.88	2.99
G*/sin δ @76°C, kPa	0.18	0.36	0.61	0.84	0.45	1.57
G*/sin δ @82°C, kPa						0.89
Tests on RTFOT residue (w=10rad/s)						
Mass Loss,%	0.82	0.41	0.57	0.53	0.64	0.39
G*/sin δ @52°C, kPa	10.99	15.86	25.81	20.00	30.22	64.82
G*/sin δ @58°C, kPa	4.54	7.23	11.76	10.65	13.31	31.47
G*/sin δ @64°C, kPa	2.04	3.48	5.99	4.64	5.63	15.00
G*/sin δ @70°C, kPa	0.91	1.89	2.71	2.43	2.77	7.74
G*/sin δ @76°C, kPa	0.45	0.93	1.37	1.34	1.30	4.05
Tests on PAV+ RTFOT residue						
G* sin δ @13°C, kPa	7975.9	4931.0	5964.0	10187.7	9128.5	6423.0
G* sin δ @16°C, kPa	5963.6	3639.0	4603.4	6860.6	7276.5	4863.6
G* sin δ @19°C, kPa	4307.0	2600.9	3339.6	4516.3	5470.0	3676.7
G* sin δ @22°C, kPa	3189.9	1846.5	2450.1	3174.8	4270.0	2791.8
G* sin δ @25°C, kPa	2205.0	1306.2	1767.4	2237.7	3083.5	2105.4
G* sin δ @28°C, kPa	1412.0	865.4	1113.2	1433.3	1900.9	1443.7
G* sin δ @31°C, kPa	877.0	550.4	703.7	912.6	1258.5	1008.0
G* sin δ @34°C, kPa	529.6	290.0	459.9	589.0	771.8	713.6
Bending Beam						
Stiffness,S,-12°C, MPa	101.2	75.9	96.1	119.1	115.9	79.4
Stiffness,S,-18°C, MPa	209.8	173.3	186.9	268.8	239.2	177.4
Stiffness,S,-24°C, Mpa	349.9	281.5	298.9	444.4	476.8	313.8
Slope, m, 60s, -12°C Slope,	0.356	0.358	0.322	0.388	0.341	0.342
m, 60s, -18°C Slope, m,	0.308	0.339	0.335	0.319	0.302	0.301
60s, -24°C	0.281	0.303	0.302	0.263	0.248	0.250
PG grade passed	PG58-28	PG64-34	PG70-34	PG70-28	PG64-28	PG76-28

3.3. Binder rheological properties at low service temperature

When an asphalt pavement surface is cooled down by weather, contraction strains are induced in the asphalt concrete. Thermal cracking will occur when these thermal contraction strains exceed the maximum fracture strain of the asphalt concrete, and is normally manifested by transverse cracks on the asphalt pavement. Many researchers [10-11] have recommended limiting viscosity or stiffness values of asphalt cement or HMA for a particular temperature range based on field experiments. A stiffness limit of 300 MPa for a loading time of 2 hours or a failure strain limit of 1.0% for an elongation rate of 1.0 mm/min has been used in the SHRP specification to reduce low temperature cracking.

In this study, three different test parameters namely Faass breaking point, creep stiffness and failure strain limit were used to evaluate the low temperature cracking potential of the asphalt mixtures. Figures 3 and 4 show the plot of predictive limiting stiffness and strain temperatures versus the Fraass breaking point for all six asphalt binders after the RTFOT and PAV processes. Predictive limiting stiffness temperature increases as the Fraass breaking point increases. The relationship is moderate ($R^2 = 0.75$). Predictive limiting strain temperature decreases as the Fraass breaking point increases.

The relationship is poor ($R^2 = 0.54$) as compared with the relationship between predictive limiting stiffness temperature and the Fraass breaking point. Figure 5 shows the plot of creep stiffness versus failure strain at -12 , -18 and -24°C for all six asphalt binders after the RTFOT and PAV processes. Creep stiffness decreases as failure strain increases. The relationship is fair ($R^2 = 0.81$) as compared with the others. The Fraass breaking points, predictive limiting stiffness temperatures, and predictive limiting strain temperatures of the

binders are shown in Table 3. The results show that the Fraass Breaking Point is $11 \sim 23^\circ\text{C}$ above the SHRP predictive cracking temperature for all six asphalt binders after the RTFOT and PAV processes.

The cracking temperature as predicted by the SHRP predictive limiting stiffness temperature is higher than the predictive limiting strain temperature.

3.4. Comparison of PG grade and bitumen test data chart

The Bitumen Test Data Chart (BTDC) consists of one horizontal scale for the temperature and two vertical scales for the penetration and viscosity, respectively. The consistency of an asphalt binder at different temperatures can be plotted on the BTDC to show its temperature susceptibility. The BTDC basically allows one to take different physical property measurements (viscosity, penetration, Fraass breaking point, and/or softening point) and, from these, predict the consistency of the material over a wide temperature range.

Additionally, it is a good idea to use family curves of the BTDC which could show the effects of aging on an asphalt binder over a wide temperature range [13]. Figures 6 through 10 show the BTDC plots of the unaged, RTFOT-aged, and PAV+ RTFOT -aged asphalt binders. The slopes of the BTDC plot show the temperature susceptibility and can be used to compare the characteristics of the aged residues with and without the original asphalt binders. It also shows that a PG grade with a wide temperature range will display less temperature susceptibility in the BTDC plots.

For example, the SBR-modified binder (PG 70-34) has lower temperature susceptibility as compared with unmodified binder (PG 58-28) at the unaged, RTFOT-aged and PAV-aged conditions.

Table 3. Test results on PAV+RTFOT-aged asphalt binders

Asphalt binders		AC-10	AC-10+ 3%SBR2	AC-10+ 3%SBR7	AC-20+ 3%SB	AC-30	AC-30+ 10%CR
Failure strain (%)	-12°C	1.378	3.848	1.683	0.965	0.834	1.514
	-18°C	0.402	1.102	0.608	0.368	0.327	0.465
	-24°C	0.360	0.581	0.365	0.307	0.286	0.294
Temperature at 1% failure strain, °C		-14.2	-19.2	-15.8	-11.7	-10.0	-14.9
Limiting strain temperature, °C		-24.2	-29.2	-25.8	-21.7	-20.0	-24.9
Limiting stiffness temperature, °C		-31.9	-35.0	-34.1	-29.1	-29.5	-33.4
Fraass breaking point, °C		-9.0	-12.5*	-12.3*	-10.8	-8.8	-9.8*
PG grade		PG58-28	PG64-34	PG70-34	PG70-28	PG64-28	PG76-28

Note: * means the first micro-crack.

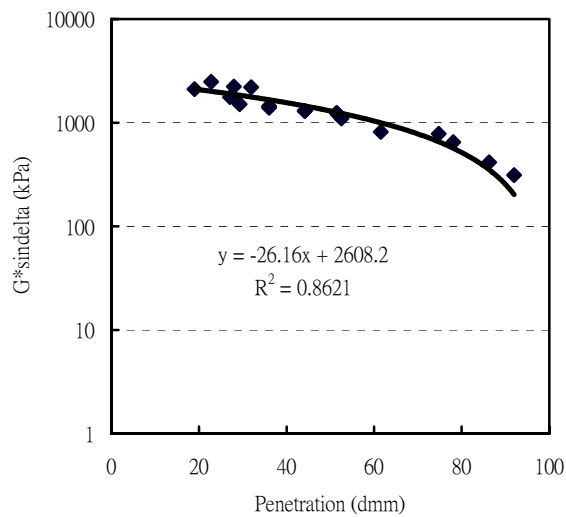


Figure 2. Relationship between penetration and $G^* \sin \delta$ before and after the RTFOT and PAV at 25°C

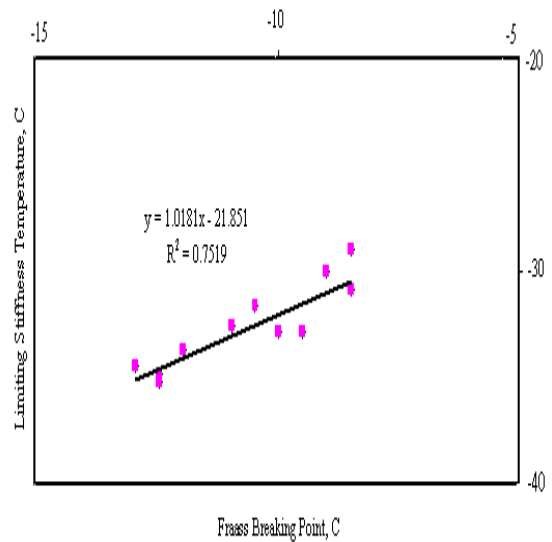


Figure 3. Relationship between Fraass breaking point and predictive limiting stiffness Temperature after the RTFOT and PAV

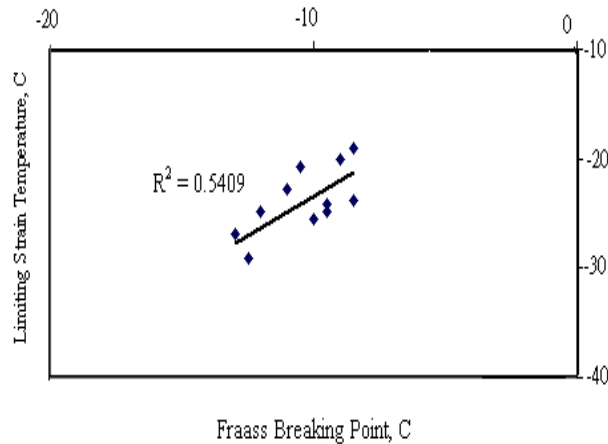


Figure 4. Relationship between Fraass breaking Point and predictive limiting strain temperature after the RTFOT and PAV

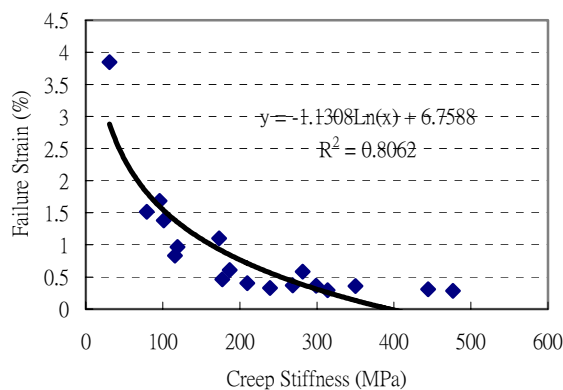


Figure 5. Relationship between creep stiffness and failure strain at -12,-18, and-24°C after the RTFOT and PAV4.

4. Summary

The main findings from this study are summarized as follows:

1. The Brookfield viscosity shows a good correlation with the $G^*/\sin\delta$ at 60°C for all

six asphalt binders before and after the RTFOT process. $G^*/\sin\delta$ increases as the viscosity increases.

2. The penetration shows a good correlation with the $G^*\sin\delta$ at 25°C for all six asphalt binders before and after the RTFOT and PAV processes. $G^*\sin\delta$ (loss modulus) increases as the penetration decreases.
3. The creep stiffness shows a good relationship with the failure strain at -12, -18 and -24°C for all six asphalt binders after the PAV process. Creep stiffness decreases as failure strain increases.
4. Faass breaking point could be used as an indicator of low temperature cracking resistance as the SHRP creep stiffness and failure strain limit. However, the cracking temperature as predicted by the Fraass breaking point is 11 ~ 23°C above the SHRP predictive cracking temperature.
5. A PG grade with a wide temperature range will display less temperature susceptibility in the BTDC. Family curves of the BTDC could be used to compare the characteristics of an asphalt binder as it ages.

References

- [1] Kennedy, T.W. and E.T. Harrigan. 1990. The SHRP Asphalt Research Program Product. *Journal of the Association of Asphalt Paving Technologists*, 59: 610-620.
- [2] Anderson, D. A., and T. W. Kennedy. 1993. Development of SHRP Binder Specification. *Journal of the Association of Asphalt Paving Technologists*, 62: 481-507.
- [3] Anderson, D.A. and Christensen, D.W. and H. Bahia. 1991. Physical Properties of Asphalt Cement and the Development of Performance-Related Specifications. *Journal of the Association of Asphalt Paving Technologists*, 60: 437-475.

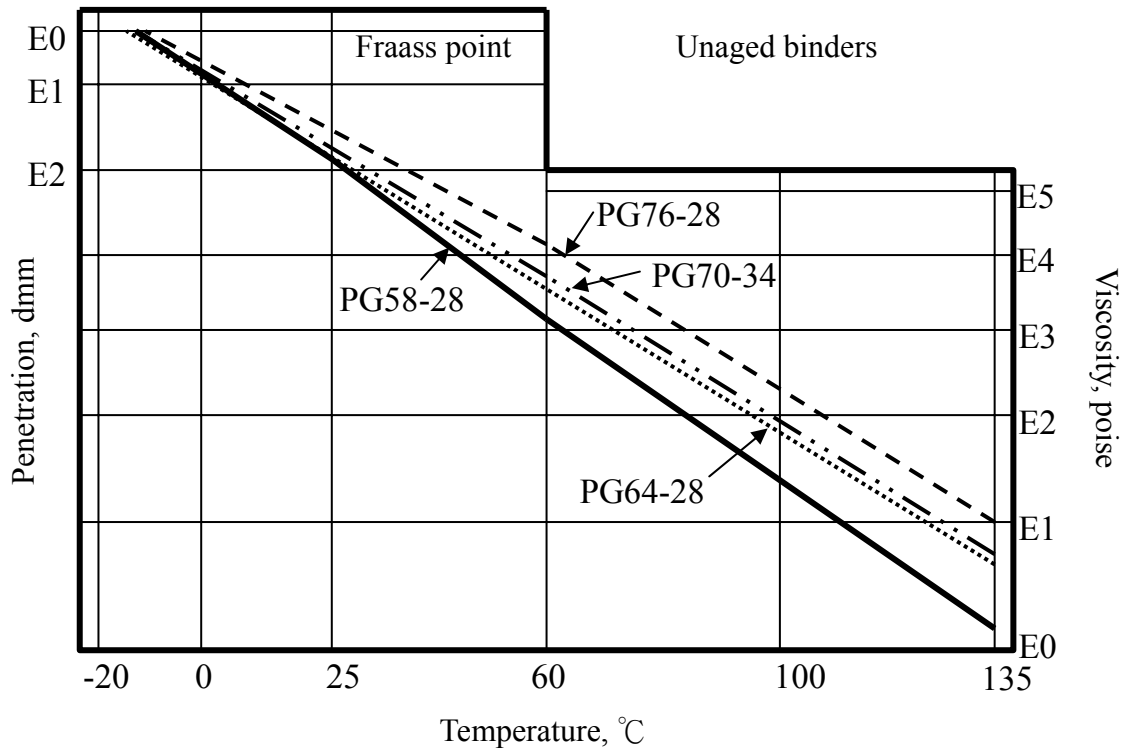


Figure 6. Bitumen test data chart for unaged asphalt binders

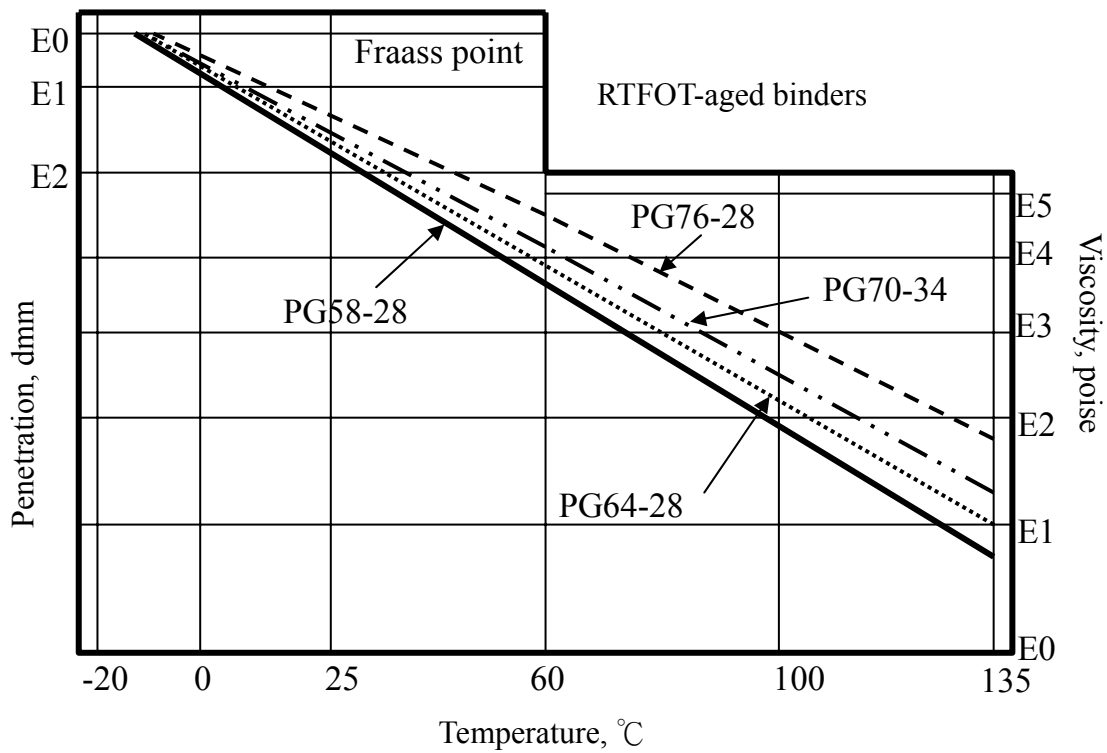


Figure 7. Bitumen test data chart for RTFOT-aged asphalt binders

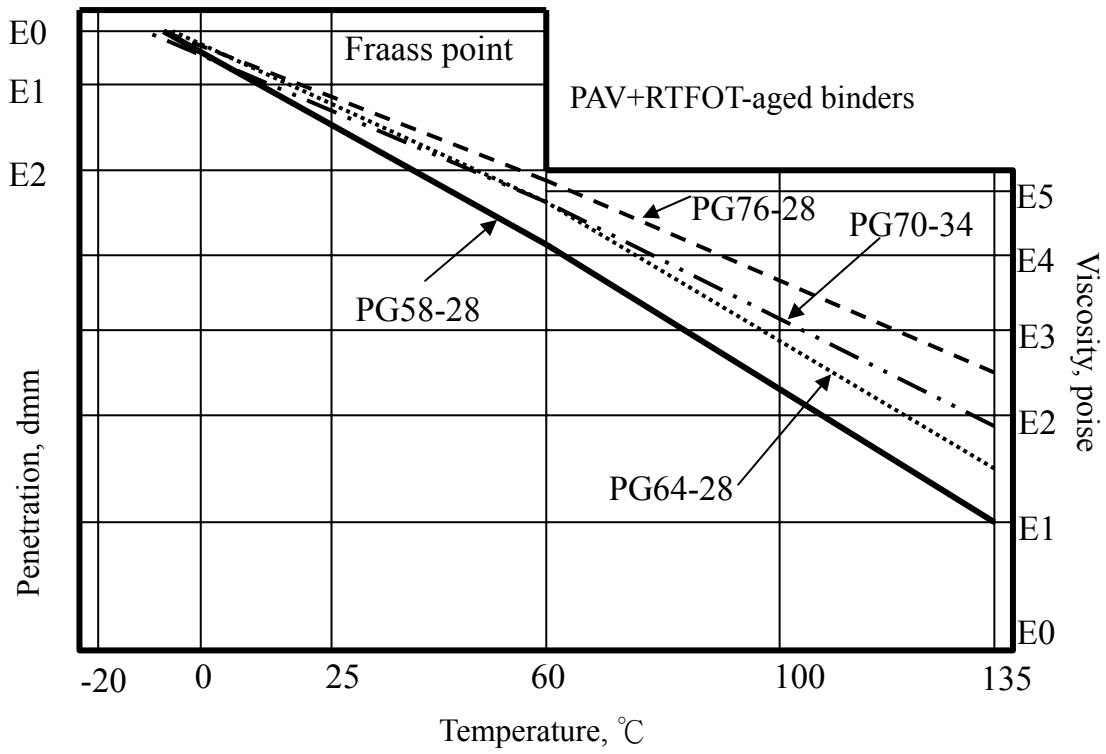


Figure 8. Bitumen test data chart for PAV+RTFOT-aged asphalt binders

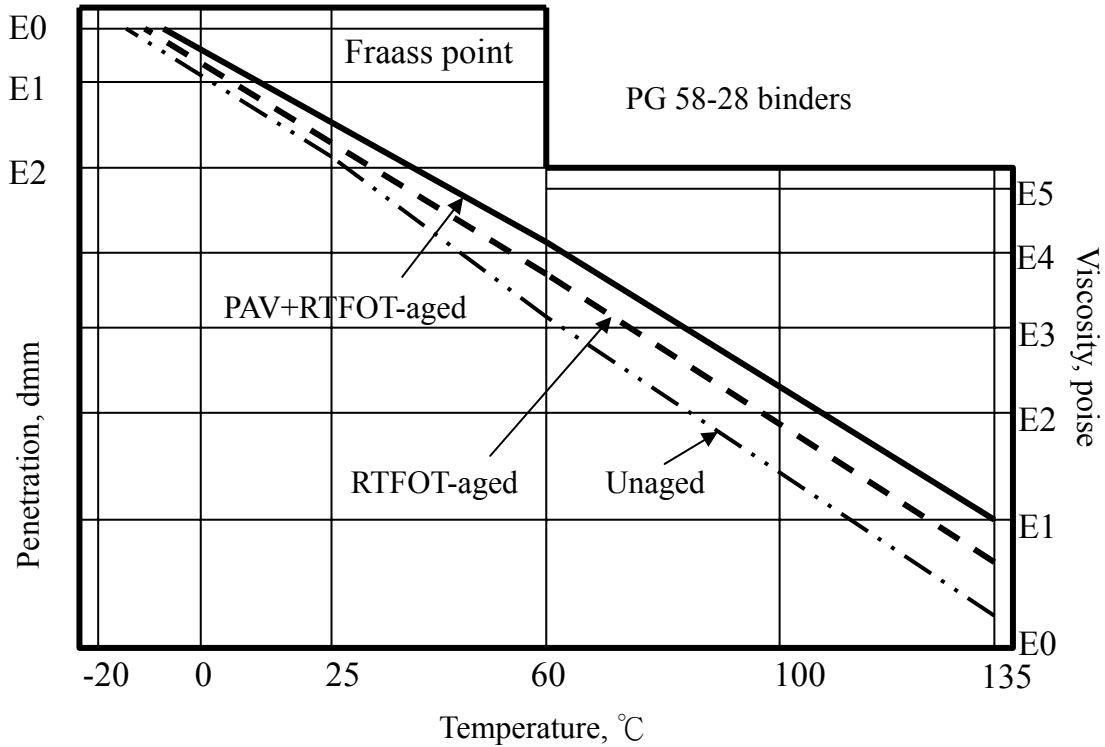


Figure 9. Bitumen test data chart for AC-10 (PG 58-28) binders

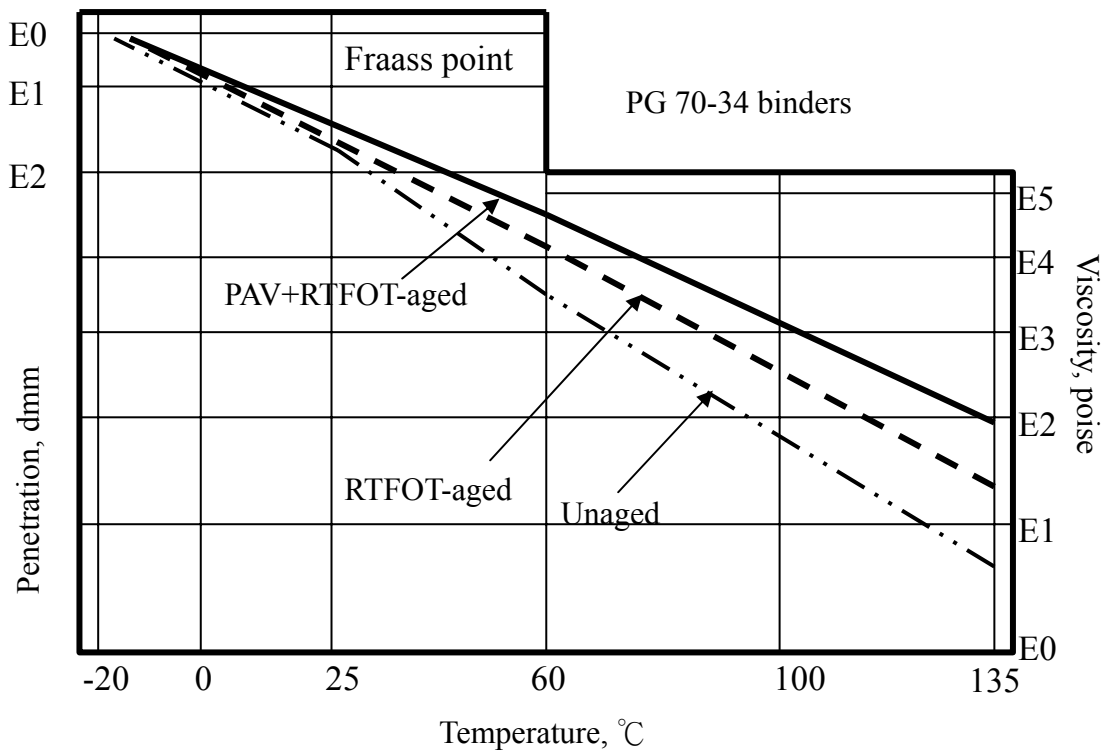


Figure 10. Bitumen test data chart for AC-10+3%SBR7(PG70-34)binders

- [4] Bell, C. A., Sosnovske, D., and J. E. Kliewer. 1994. Relating Asphalt and Aggregate Properties and their Laboratory Aging to Field Performance of Asphalt Mixtures. *Paper presented at the 73rd Annual Meeting of Transportation Research Board, Washington, D.C.*
- [5] Reese, R. 1994. Development of a Physical Property Specification for Asphalt-Rubber Binder. *Journal of the Association of Asphalt Paving Technologists*, 63.
- [6] Bahia, H. U. and D.A. Anderson. 1995. The SHRP Binder Rheological Parameters: Why are They Required and How do They Compare to Conventional Properties. *A paper presented at the 74th Annual Meeting of Transportation Research Board, Washington, D. C.*
- [7] Tayebali, A., Deacon, J. Coplantz, J. and C. Monismith. 1993. Modeling Fatigue Response of Asphalt-Aggregates Mixtures. *Journal of the Association of Asphalt Paving Technologists*, 62.
- [8] Pell, P. S. and K. E. Cooper. 1975. The Effect of Testing and Mix Variables on the Fatigue Performance of Bituminous Materials. *Journal of the Association of Asphalt Paving Technologists*, 44: 1-37.
- [9] Anderson, D.A. and D.W. Christensen. 1992. Interpretation of Dynamic Mechanical Test Data for Paving Grade Asphalt Cements. *Journal of the Association of Asphalt Paving Technologists*, 61: 67-116.
- [10] Chen, J. S. and C. H. Lin. 2003. Establishing Viscoelastic Model of Hot-Mix Asphalt Mixture and its Relationship to Pavement Performance. *Journal of Chinese Institute of Civil and Hydraulic Engineering*, 15, 1: 169-180.
- [11] Tia, M. 2002. Evaluation of Superpave Mixtures with and without SBS Modification by means of Accelerated Pavement Testing. *An invited paper presented at the 5th National Pavement Recycling Conference, R. O. C.*

- [12] Kan, Y. C. and M. G. Lee. 2002. A Study of Crumbed Scrap Tire being Applied to Concrete Construction. *Journal of Chinese Institute of Civil and Hydraulic Engineering*, 14, 1: 141-149.
- [13] Lee, M. G. 1996. *Development of Relationships Between SHRP Asphalt Test Parameters and Structural Mixtures for Mechanistic Analysis and Rehabilitation Design of Flexible Pavements*. Ph.D. Dissertation, University of Florida.
- [14] Yoshida, Junko. 2004. MIPS to focus on digital camera market. *Technical Paper; EE Times*.